

Preparation and structural characterization of sol-gel-derived silver silica nanocomposite powders

Duy Phong Pham¹, Kim Khanh Huynh², Cao Vinh Tran¹, Van Quang Vu³,
Thi Thanh Van Tran^{2,*}

¹Laboratory of Advanced Materials, University of Science, Vietnam National University Ho Chi Minh City, Vietnam

²Faculty of Materials Science, University of Science, Vietnam National University Ho Chi Minh City, Vietnam

³International Training Institute for Material Science (ITIMS), Hanoi University of Science and Technology (HUST), Hanoi, Vietnam

Email address:

pdphong@hcmus.edu.vn (D. P. Pham), tttvan@hcmus.edu.vn (T. T. V. Tran)

To cite this article:

Duy Phong Pham, Kim Khanh Huynh, Cao Vinh Tran, Van Quang Vu, Thi Thanh Van Tran. Preparation and Structural Characterization of Sol-Gel-Derived Silver Silica Nanocomposite Powders. *International Journal of Materials Science and Applications*.

Vol. 3, No. 5, 2014, pp. 147-151. doi: 10.11648/j.ijmsa.20140305.13

Abstract: The silver embedded silica powders (Ag/SiO₂) have been successfully prepared by sol-gel method. Ag nanoparticles were formed from the thermal decomposition of the silver nitrate. X-ray diffraction shows that the silver nanocrystals have appeared after a heat-treatment at 600 °C. TEM images show that the spherical silver particles with an average size around 30 nm dispersed homogeneously in silica matrix. The data of XRD, Raman and FTIR spectroscopy prove that the formation of the silver nanocrystals influent on the structural evolution of the silica matrix. The presence of metal nanocrystals leads to remarkable decrease in crystallizing temperature of SiO₂. In addition, the adsorption-desorption analysis indicated that the growth of Ag particles makes the pores in silica structure widen.

Keywords: Silver Nanoparticles, Silica Phase Transformation, Raman Spectroscopy, Ag/SiO₂ Nano-Composite

1. Introduction

The nanocrystal silver particles have attracted the attention due to their widely potential applications in many fields such as catalysts, optoelectronics, the surface enhanced Raman scattering (SERS), chemical and biological sensing and especially known as the most common antibacterial materials¹⁻⁴. The silver nanoparticles have been introduced into many different inorganic materials as SiO₂, TiO₂, ZnO, SiO₂-TiO₂⁵⁻⁸. Of these, Ag-loaded SiO₂ (Ag/SiO₂) has been known for its high chemical durability, safety and heat resistance. In addition, the SiO₂ materials, known as porous structure, can adsorb various ions and organic molecules easily in its pores and on its surfaces. Because of this, it is expected to be one of the most promising carriers suitable for development of high performance antibacterial and bactericidal materials⁹. There are a lot of methods used to prepare Ag/SiO₂ nano-composites including sol-gel, sputtering, ion implantation, ion exchange, high-temperature glass fusion, etc.^{8,10-12}. Among these methods, the sol-gel has several advantages such as high purity, ultra-homogeneity, low

synthesis temperature, and most significantly the possibility of making glasses of new compositions¹³.

In order to prevent the aggregation of silver nanoparticles (NPs) into clusters the protecting agents or stabilizers, which are amphiphilic, polymer polyvinyl pyrrolidone (PVP)¹⁴, poly(vinyl alcohol) (PVA)¹⁵, Sodium Dodecyl Sulphate (SDS), or Citrate of sodium¹⁶, were used in synthesis process. However, these additional agents can result in complex synthesis process, toxicity, and higher cost. That why a synthesis process without PVP, PVA or SDS attracts attention for economic industrial applications.

A silica matrix also can be used as an agent in order to prevent the aggregation of silver particles. Moreover, due to the unknown health risks of metal NPs, they are necessary to be tightly attached; hence their diffusion to the environment is inhibited. Many authors prepared silver nanoparticles in silica matrix under different forms such as rods¹⁷, powders^{11,18} or monoliths^{19,20} for antibacterial applications.

This work presents a collection of data obtained for sol-gel-derived SiO₂-5mol% silver nano-composites powders without protecting agents, which are developed for applications in antibacterial and environment. In this study,

the formation of silver crystals as a function of annealing temperatures and their effect on the structural evolution of silica matrix were also demonstrated.

2. Experiment

2.1. Sample Preparation

Ag/SiO₂ nano-composite powders with 5 mol% silver were prepared by sol-gel method. The precursors consisted of tetraethyl orthosilicate (TEOS, Si(OC₂H₅)₄, Merck), silver nitrate (AgNO₃, Merck), ethanol (C₂H₅OH, Merck), nitric acid (HNO₃, Merck), and distilled water. The molar ratio of TEOS: C₂H₅OH: HNO₃: H₂O was 1: 4: 0.15: 10, respectively. In the first step, amount of AgNO₃ and distilled water were mixed and stirred for 30 min at room temperature to form A-solution. In another beaker, TEOS and ethanol were also mixed for 30 minutes to obtain B-solution. Then, B-solution was slowly poured into A-solution under stirring. After 30 min stirring, this mixture was added by HNO₃, ethanol and H₂O. The finally mixed solution was continuously stirred for 4 hours at room temperature and then placed into sealed polypropylene containers. The gelation occurred in air after one week. The obtained bulk samples were grinded into fine powders. These powders were annealed in air at various temperatures from 300 °C to 1000 °C for 1 hour.

2.2. Characterization

The crystalline phases of the powders were characterized by XRD patterns using a D8 Advance (Bruker) X-ray diffractometer (XRD) with Cu K α radiation ($\lambda = 0.154$ nm). The morphology of samples were recorded by the transmission electron microscopy (TEM, JEM-1400, Japan).

The pore sizes and the distributions of pores as well as the specific surface area were deduced from the nitrogen adsorption and desorption measurements according to BJH model using Micromeritics porosimeter.

The effect of annealing temperatures and silver nanocrystals on the structural evolution of silica matrix were studied by spectroscopic measurements. The IR transmission were examined by EQUINOX 55 (BRUKER) in the range of 4000-400 cm⁻¹ using potassium bromide (KBr)-based pellets. These pellets were prepared by mixing KBr powder and Ag-SiO₂ powder with a ratio of 130:1, respectively. By using a Renishaw instrument, Raman spectra of powders under an excitation wavelength at 633nm were recorded.

3. Results and Discussion

3.1. Crystallization of Silver and Silica

X-ray diffraction patterns of powders annealed from 400 °C to 1000 °C are revealed in Fig. 1. It is seen that no peaks characterized for silver crystal phase are present at temperatures below 500 °C. After a heat-treatment at 600 °C,

the appearance of a weak peak at $2\theta = 38^\circ$ is assigned to the (111) planes of silver crystals. At higher temperatures, in addition to the peak at 38°, peaks at $2\theta = 44.6, 64.6$ and 77° , which correspond to (200), (220), and (311) planes of silver face-centered cubic phase (JCPDS No. 04-0783), appear clearly. The increase in intensity of peaks with annealing temperatures, accompanied by a decrease in peak width, attests to the increase in grain size.

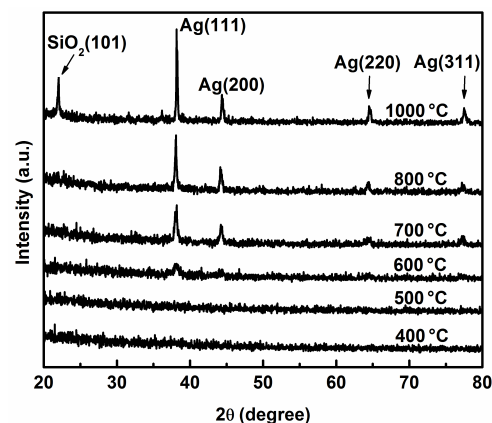


Figure 1. XRD patterns of the SiO₂-5% Ag powders heat-treated at different temperatures for 1 h.

The average diameter of the silver particles was calculated from the diffraction peaks using Scherrer's formula:

$$D = \frac{0.9\lambda}{\beta \cdot \cos \theta}$$

where D is mean crystallite size, β is the width of the peak at half maximum intensity of a specific phase in radians, and λ is the wavelength of incident rays, θ is the center angle of the peak in radian. The mean crystallite size for silver nanoparticles was evaluated to be 20 and 35 nm for samples heat-treated at 600° and 1000°C, respectively.

Moreover, the appearance of a new intense peak at $2\theta = 22^\circ$ in the top diffraction pattern is assigned to (101) planes in cristobalite structure of silica. This observation denotes that the crystallization of silica occurs around 1000 °C, while that of pure silica systems begins at 1400 °C²¹. It is suggested that the presence of metallic silver particles favors crystallization of sol-gel derived silica. According to the model suggested by L. L. Díaz-Flores *et al.*, the near-to-metal atoms of a matrix will be in the vibrational state much different from the bulk atoms. This vibrational energy is sufficient to break the inter-atomic bonds, thus disrupting the amorphous network and reducing the kinetic barrier to the crystallization^{21,22}.

A TEM image of the 5 mol% Ag powder heat-treated at 800°C is presented in Fig.2. showing a relatively homogenous distribution of Ag spherical particles throughout the amorphous silica network. In the studies of a very large number of images for 5 mol% Ag systems, the particle sizes range between 20 and 40 nm for samples

heat-treated at 800°C. This value correlates with that obtained from XRD data.

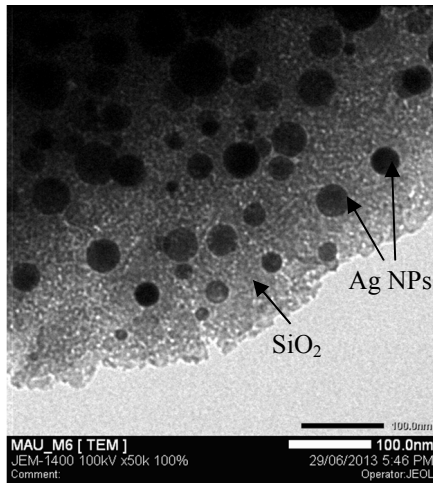


Figure 2. TEM images of a SiO₂-5%Ag sample after a heat-treatment at 800 °C for 1h

3.2. Structural Evolutions of Silica Matrix

3.2.1. FTIR Spectroscopy

Fourier transform infrared spectroscopy (FT-IR) was used to investigate the structural change of SiO₂ as a function of annealing temperatures.

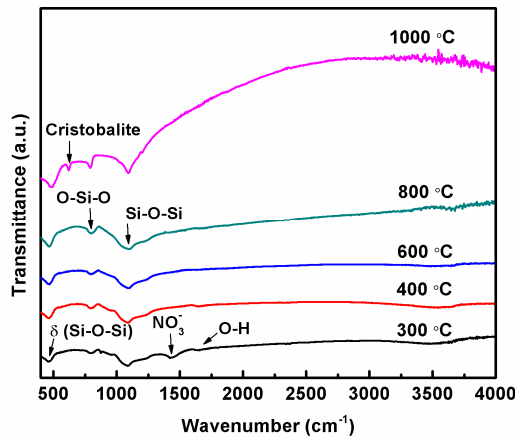


Figure 3. FT-IR spectra of the SiO₂-5% Ag powders heat-treated at different temperatures for 1h

Fig. 3 shows the FT-IR transmission spectra for 5 mol% powder samples heat-treated at various temperatures. The broad band observed around 3458 cm⁻¹ and that at 1643 cm⁻¹ are typical of vibrational modes involving O-H groups of residual water and alcohol groups. The disappearance of O-H groups at annealed temperatures above 600 °C confirms the elimination of hydroxyl or organic groups in the densified powders. The band at 1429 cm⁻¹ is attributed to NO₃⁻ ions¹³. The gradual decrease of NO₃⁻ ions upon further increased annealing temperatures can be due to the strongly happened pyrolysis process of AgNO₃, releasing the Ag atoms and NO₂ gas. The strong band at 1088 cm⁻¹ along with the accompanying shoulder at 1228 cm⁻¹ is the asymmetric

stretching vibration of Si—O—Si bonds linking of the SiO₂ tetrahedra; the band at 804 cm⁻¹ is assigned to O—Si—O modes, while the band at 454 cm⁻¹ corresponds to the δ (Si—O—Si) bending mode¹³. With increasing annealing temperatures, no displacements to higher wavenumbers of all the bands related to polyhedral vibrations imply that the growing crystalline NPs have no effect on the densification of the SiO₂ matrix. However, a particular attention in FTIR analysis was the appearance of new peak at 620 cm⁻¹ in the spectra of powder annealed at 1000°C and the peaks at 1100cm⁻¹, 792cm⁻¹ and 490 cm⁻¹ become narrower. This behavior is related to cristobalite phase of silica²³, which proves that crystallization of silica occurs at 1000 °C in the silver silica nanocomposites. This observation is completely identical with XRD data.

3.2.2. Raman Spectroscopy

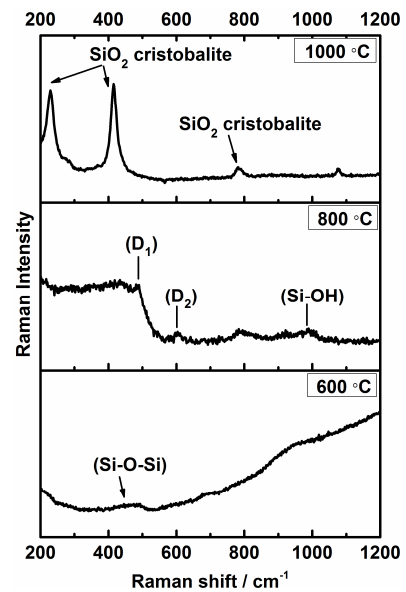


Figure 4. Raman spectra of the samples annealed at 600 °C, 800 °C and 1000 °C for 1h

Raman techniques were also used to study the structural evolutions of silica matrix caused by the presence of silver particles as a function of the annealing temperatures. Fig. 4 shows the Raman spectra of the powders heat-treated at temperatures ranging from 600 °C to 1000 °C. For the sample heat-treated at 600 °C, the great quantity of residual organic reactants in the samples was able to result in a high level of spectral fluorescence. The featured bands for the amorphous nature of silica were observed in the system heat-treated at 800 °C. The band at 440 cm⁻¹ is attributed to bending mode of Si-O-Si. The D₁ and D₂ bands at 487 and 602 cm⁻¹, are assigned to symmetric breathing modes of four-membered and three-membered rings of SiO₂ tetrahedra, respectively. The band at 783 cm⁻¹ corresponds to the motion of silicon against its tetrahedral oxygen cage. Finally, the band at 980 cm⁻¹, which is related to vibrations of Si-OH groups²⁴, decreases in intensity with increasing annealing temperatures indicating the gradual removal of the

solvent and precursor molecules.

It can be seen that there is a remarkable change in the spectral features between samples heated at 800 °C and 1000 °C. In the top spectrum, the appearance of the most intense peaks centered at 230cm^{-1} , 416cm^{-1} and the least significant at 784cm^{-1} can be interpreted as signatures of the SiO_2 cristobalite structure²³. This observation confirms clearly that the phase transformation of silica occurs at 1000 °C. This finding supports the results from the XRD and FTIR analysis, as has been described previously.

3.3. Textural Properties

In order to verify the effect of the growth of silver crystals on the porosity of the xerogels, nitrogen adsorption-desorption isotherms were recorded.

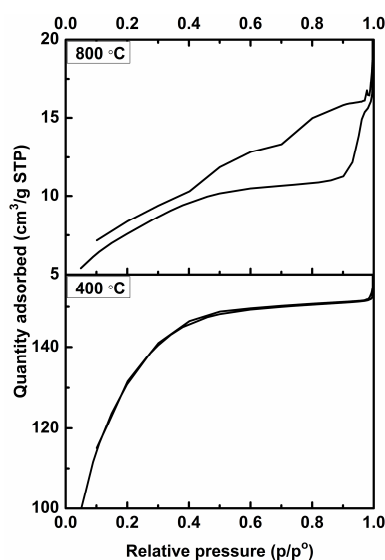


Figure 5. Nitrogen adsorption-desorption isotherms for the SiO_2 -5% Ag powder heat-treated at 400 °C and 800 °C for 1h

From Fig. 5, it can be clearly seen that the nitrogen adsorption isotherm of the sample heat-treated at 400 °C can be classified as type I, which is typical for microporous adsorbent. However, a type-IV isotherm is observed for the powder annealed at 800 °C (according to IUPAC classification). In the latter case, the isotherm exhibits a hysteresis loop, i.e. the adsorption and desorption isotherms do not coincide over a certain region of external pressures. This loop is characteristic of mesoporous samples with interconnected pores. The analysis of the adsorption-desorption isotherms shows that the average pore diameter after a calcination at low temperature remains at about 22 Å, while this value reaches 39Å in the system treated at higher heat-treatment. The TEM and XRD analyses illustrated that the increase in annealing temperature induces precipitation of bigger silver nanoparticles in the pores of silica. The presence and coarsening of Ag particles within channels of pore or between pores result in more and more isolated and unmeasured free spaces. That is the reason that the size of pores for the sample annealed at 800 °C is nearly twice as

large as that of pores after heated at 400 °C. This increment leads to remarkable decrease of surface area from $433.8\text{m}^2/\text{g}$ to $27.7\text{m}^2/\text{g}$.

4. Conclusion

Using a sol-gel technique, the Ag/ SiO_2 nanocomposites have been successfully fabricated without protecting agents. TEM data present a relatively homogenous distribution of spherical silver nanoparticles throughout the amorphous silica network and the size ranges between 20 and 40 nm after a heat-treated at 800 °C for 1h in air. Combination of XRD and TEM analyses with data of FT-IR and Raman spectroscopies show that the formation of silver nanocrystals results in significant decrease in crystalline temperature of silica matrix. In addition, the growth of silver particles with annealing temperatures has no effect on the densification of silica and leads to decrease the specific surface area. These powders will be the potential materials for antibacterial activity.

Acknowledgement

This work was supported by the Advanced Materials Laboratory, HCMC University of Science, Vietnam National University and International Training Institute for Materials Science, Ha Noi University of Science and Technology.

References

- [1] R. J. Chimentão, I. Kirm, F. Medina, X. Rodríguez, Y. Cesteros, P. Salagre, J. E. Sueiras, J. L. G. Fierro, "Sensitivity of styrene oxidation reaction to the catalyst structure of silver nanoparticles" *Appl. Surf. Sci.*, vol. 252, pp. 793–800, 2005.
- [2] N. Baheiraei, F. Moztarzadeh, and M. Hedayati, "Preparation and antibacterial activity of Ag/ SiO_2 thin film on glazed ceramic tiles by sol-gel method", *Ceram. Int.*, vol. 38, pp. 2921–2925, 2012.
- [3] L. Guo, A. Guan, X. Lin, C. Zhang, and G. Chen, "Preparation of a new core-shell Ag@ SiO_2 nanocomposite and its application for fluorescence enhancement", *Talanta* vol. 82, pp. 1696–1700, 2010.
- [4] S. Long, L. Li, H. Guo, W. Yang, and F. Lu, "Preparation of stable core-shell dye adsorbent Ag-coated silica nanospheres as a highly active surfaced-enhanced Raman scattering substrate for detection of rhodamine 6G", *Dye. Pigment*, vol. 95, pp. 473–477, 2012.
- [5] P. Amornpitoksuk, S. Suwanboon, S. Sangkanu, A. Sukhoom, N. Muensit, and J. Baltrusaitis, "Synthesis, characterization, photocatalytic and antibacterial activities of Ag-doped ZnO powders modified with a diblock copolymer", *Powder Technol.*, vol. 219, pp. 158–164, 2012.
- [6] B. Sun, S. Sun, T. Li, and W. Zhang, "Preparation and antibacterial activities of Ag-doped SiO_2 - TiO_2 composite films by liquid phase deposition (LPD) method", *J. Mater. Sci.*, vol. 42, pp. 10085–10089, 2007.

- [7] N. Sobana, M. Muruganadham, and M. Swaminathan, "Nano-Ag particles doped TiO₂ for efficient photodegradation of direct azo dyes". *J. Mol. Catal. A Chem.*, vol. 258, pp. 124–132, 2006.
- [8] M. Kawashita, S. Tsuneyama, F. Miyaji, T. Kokubo, H. Kozuka, and K. Yamamoto, "Antibacterial silver-containing silica glass prepared by sol-gel method", *Biomaterials*, vol. 21, pp. 393–398, 2000.
- [9] H. Jia, W. Hou, L. Wei, B. Xu, and X. Liu, "The structures and antibacterial properties of nano-SiO₂ supported silver/zinc-silver materials", *Dent. Mater.*, vol. 24, pp. 244–249, 2008.
- [10] S. Duhan, S. Devi, and M. Srivastava, "Characterization of nanocrystalline Ag/SiO₂ nanocomposites and synthesis by wet chemical method", *Indian J. Pure Ap. Phy.*, vol. 48, pp. 271–275, 2010.
- [11] B. Mahltig, H. Haufe, K. Muschter, A. Fischer, Y.H. Kim, E. Gutmann, M. Reibold, D.C. Meyer, T. Textor, C.W. Kim, and Y.S. Kang, "Silver nanoparticles in SiO₂ microspheres - preparation by spray drying and use as antimicrobial agent". *Acta Chim. Slov.* vol. 57, pp. 451–457, 2010.
- [12] Y.K. Mishra, S. Mohapatra, D. Kabiraj, B. Mohanta, N.P. Lalla, J.C. Pivin, and D.K. Avasthi, "Synthesis and characterization of Ag nanoparticles in silica matrix by atom beam sputtering", *Scr. Mater.*, vol. 56, pp. 629–632, 2007.
- [13] H.-J. Jeon, S.-C. Yi, and S.-G. Oh, "Preparation and antibacterial effects of Ag–SiO₂ thin films by sol–gel method", *Biomaterials*, vol. 24, pp. 4921–4928, 2003.
- [14] K. S. Chou, C. C. Chen, "Fabrication and characterization of silver core and porous silica shell nanocomposite particles", *Micropor. Mesopor. Mat.*, vol. 98, pp. 208–213, 2007.
- [15] A. A. El-kheshen, S. F. G. El-rab, "Effect of reducing and protecting agents on size of silver nanoparticles and their anti-bacterial activity", *Der. Pharma. Chemica.*, vol. 4, pp. 53-65, 2012.
- [16] M. G. Guzmán, J. Dille, S. Godet, "Synthesis of silver nanoparticles by chemical reduction method and their antibacterial activity", *Int. J. Chem. Biomolecular Eng.*, vol. 2-3, pp. 104–111, 2009.
- [17] A. Chahadih, H. El Hamzaoui, O. Cristini, L. Bigot, R. Bernard, C. Kinowski, M. Bouazaoui, B. Capoen, "H₂-induced copper and silver nanoparticle precipitation inside sol-gel silica optical fiber preforms" *Nanoscale Res. Lett.*, vol. 7, pp. 487, 2012.
- [18] A. Hilonga, J. K. Kim, P. B. Sarawade, D. V. Quang, G. Shao, G. Elineema, H. T. Kim, "Silver-doped silica powder with antibacterial properties", *Powder Technol.*, vol. 215-216, pp. 219–222, 2012.
- [19] Surender Duhana, N. Kishoreb, P. Aghamkarc, Sunita Devi, "Preparation and characterization of sol–gel derived silver-silica nanocomposite", *J. Alloys and Compounds*, Vol. 57, pp. 101-104, 2010.
- [20] D. C. Ram, "Microstructure and surface morphology of nanocrystalline silver silicates", *Acta Physica Polonica A*, vol. 121, pp. 2000–2002, 2012.
- [21] L. L. Díaz-Flores, M. G. Garnica-Romo, J. González-Hernández, J. M. Yáñez-Limón, P. Vorobiev, Y. V. Vorobiev, "Formation of Ag-Cu nanoparticles in SiO₂ films by sol-gel process and their effect on the film properties", *Phys. Status Solidi*, vol. 4, pp. 2016–2020, 2007.
- [22] B. Akkopru, C. Durucan, "Preparation and microstructure of sol-gel derived silver-doped silica", *J. Sol-Gel Sci. Technol.*, vol. 43, pp. 227–236, 2007.
- [23] J. Mitra, M. Ghosh, R. K. Bordia, A. Sharma, "Photoluminescent electrospun submicron fibers of hybrid organosiloxane and derived silica", *RSC Adv.*, vol. 3, pp. 7591, 2013.
- [24] T. T. Van Tran, T. Si Bui, S. Turrell, B. Capoen, P. Roussel, M. Bouazaoui, M. Ferrari, O. Cristini, C. Kinowski, "Controlled SnO₂ nanocrystal growth in SiO₂-SnO₂ glass-ceramic monoliths", *J. Raman Spectrosc.*, vol. 43, pp. 869–875, 2012.